# Comparison of methods for the fabrication and the characterization of polymer self-assemblies: what are the important parameters ?

*Mouwanga Dionzou*[a], *Andrew Morère*[a], *Clément Roux*[a,b], *Barbara Lonetti*[a], *Jean-Daniel Marty*[a], *Christophe Mingotaud*[a], *Pierre Joseph*[b,c], *Dominique Goudounèche*[d], *Bruno Payré*[d] *Marc Léonetti*[e] , *Anne-Françoise Mingotaud*[a,]*

**Content of the supplementary information:**

- Table S1: Characterization of the polymers used
- Experimental procedures for analyses
- Table S2. Calculation of $MCH_2$ and hydrophilic fraction according to Discher
- Scheme S1. Polymers used in this study
- TEM for acetone cosolvent method
- Acetonitrile cosolvent method
- TEM for "THF/MeOH cosolvent method"
- TEM for "Meng method"
- TEM for film rehydration method
- Prevision of self-assembly morphologies
- PCA analysis
- Special cases of "PEO5000-PCL75000" and "PEO1400-PMMA5600"
- Theoretical background of Dynamic Light scattering (DLS)
- Typical optical microscopy pictures of electroformed polymersomes

| Announced polymers | Announced EO weight fraction | Announced molecular weight | Measured $M_w$ from SEC | Measured $M_n$ from SEC | Measured $M_n$ from $^1H$ NMR | $f_{PEO}$ exp | Polymer name |
|---|---|---|---|---|---|---|---|
| PEO5000-PCL75000 | 0.06 | 80000 | 31700 | 20800 | 5000-75500 | 0.06 | - |
| PEO5000-PCL37000 | 0.12 | 42000 | 33700 | 26000 | 5000-33300 | 0.13 | PEO5000-PCL33300 |
| PEO2000-PCL13500 | 0.13 | 15500 | 19800 | 16400 | 2000-13300 | 0.13 | PEO2000-PCL13300 |
| PEO2000-PCL11500 | 0.15 | 13500 | 10700 | 7900 | 2000-5800 | 0.26 | PEO2000-PCL5800 |
| PEO2000-PCL8500 | 0.19 | 10500 | 14940 | 13100 | 2000-8800 | 0.19 | PEO2000-PCL8800 |
| PEO2000-PCL7000 | 0.22 | 9000 | 8600 | 8100 | 2000-6700 | 0.23 | PEO2000-PCL6700 |
| PEO5000-PCL11000 | 0.31 | 16000 | 13700 | 12800 | 5000-10800 | 0.32 | PEO5000-PCL10800 |
| PEO11000-PMMA64000 | 0.15 | 75000 | 90800 | 69900 | 11000-66500 | 0.14 | PEO11000-PMMA66500 |
| PEO5000-PMMA22000 | 0.18 | 27000 | 29710 | 28900 | 5000-21500 | 0.19 | PEO5000-PMMA21500 |
| PEO1400-PMMMA5600 | 0.2 | 7000 | 8700 | 7000 | 1400-5600 | 0.2 | PEO1400-PMMA5600 |
| PEO5000-PMMA12300 | 0.29 | 17300 | 18100 | 16600 | 5000-11900 | 0.30 | PEO5000-PMMA11900 |
| PEO2000-PMMA5000 | 0.29 | 7000 | 8500 | 7800 | 2000-5040 | 0.28 | PEO2000-PMMA5040 |
| PEO5000-PMMA4000 | 0.56 | 9000 | 9200 | 8400 | 5000-4100 | 0.55 | PEO5000-PMMA4100 |
| PEO5000-PDLLA22000 | 0.18 | 27000 | 19300 | 17100* | 5000-20500 | 0.20 | PEO5000-PDLLA20500 |
| PEO2000-PDLA6000 | 0.25 | 8000 | 8790 | 5040 | 2000-5450 | 0.27 | PEO2000-PDLA5450 |
| PEO5000-PDLLA12000 | 0.29 | 17000 | 9250 | 7250* | 5000-10550 | 0.32 | PEO5000-PDLLA10550 |
| PEO10000-PLLA17500 | 0.36 | 27500 | 18600 | 12100* | 10000-12800 | 0.44 | PEO10000-PLLA12800 |
| PEO10000-PDLLA15000 | 0.4 | 25000 | 22900 | 18300* | 10000-17650 | 0.36 | PEO10000-PDLLA17650 |
| PEO15000-PS36000 | 0.29 | 51000 | 54700 | 53500 | 15000-37300 | 0.29 | PEO15000-PS37300 |
| PEO900-PBD1900 | 0.32 | 2800 | 3100 | 2900 | 900-2300 | 0.28 | PEO900-PBD2300 |
| PEO1300-PBD2500 | 0.34 | 3800 | 6300 | 6100 | 1300-2100 | 0.38 | PEO1300-PBD2100 |
| PEO2000-PBD3800 | 0.34 | 5800 | 11400 | 8100 | 2000-3800 | 0.34 | PEO2000-PBD3800 |
| PEO3900-PBD6500 | 0.37 | 10400 | 9240 | 9000 | 3900-6700 | 0.37 | PEO3900-PBD6700 |
| PEO1500-PBD2500 | 0.37 | 4000 | 6700 | 6200 | 1500-2300 | 0.39 | PEO1500-PBD2300 |
| PCL5900-PEO5000-PCL5900 | 0.3 | 16800 | 12280 | 10000 | 12300-5000-12300 | 0.17 | PCL12300-PEO5000-PCL12300 |
| PCL8000-PEO10000-PCL8000 | 0.38 | 26000 | 24000 | 18200 | 8250-10000-8250 | 0.38 | PCL8250-PEO10000-PCL8250 |
| PCL4500-PEO10000-PCL4500 | 0.53 | 19500 | 18240 | 14400 | 4400-10000-4400 | 0.53 | PCL4400-PEO10000-PEO4400 |
| PMOXA1200-PDMS4500-PMOXA1200 | 0.35 | 6900 | 5200 eq PMMA | 4500 eq PMMA | 1500-4500-1500 | 0.4 | PMOXA1500-PDMS4500-PMOXA1500 |

* Bi- or multimodal

**Table S1**. Characterization of the polymers used

**Polymer characterizations**. The average molecular weight of the polymers was determined by size exclusion chromatography (SEC) analysis in THF (flow rate 1.0 mL.min$^{-1}$) on an apparatus equipped with an Optilab Wyatt refractive index detector, a Waters column pack (Ultrastyragel $10^4$, $10^3$, 100 Å) and a Minidawn Wyatt light scattering detector. Molecular weights were measured using an estimated dn/dc value for the block copolymers based on known values of the weighted weight-fraction average of dn/dc for the corresponding homopolymers. $^1$H NMR spectra were recorded on a Bruker Avance 300 spectrometer and deuterated chloroform was used as solvent. Pulse delays of 5 or 10 s were used. The molecular weight of the polymers was determined based on the ratio between the ethylene oxide units and those of the hydrophobic block. For some of them, a more thorough analysis was performed to check the ethylene oxide block length by longer accumulation in order to integrate the chain ends. From the exact weight data, the $\mathbf{f_{PEO}}_{\text{exp}}$ parameter defined as the average molecular weight of PEO blocks divided by the total average molecular weight of the polymer was estimated for each polymer. Although different methods of calculating the molecular weights led to typical accuracy of 10-20%, the estimated error on $\mathbf{f_{PEO}}_{\text{exp}}$ remained below 10%. The polymers thereafter are named according to their measured NMR molecular weights, as listed in Table S1. As discussed in the text, although the formation process of the self-assemblies was not under thermodynamic equilibrium, the nano-objects formation was found to be reproducible.

**Electroformation**. A 5 mg.mL$^{-1}$ polymer solution in chloroform was prepared and 20 µL spread onto ITO-covered glass slides from Sigma (resistivity: 8-12 Ω.sq$^{-2}$). After evaporation of the solvent with a vacuum pump during approximately 30 minutes, the electroformation chamber made of two slides spaced by 1 mm was filled with 50 to 250 mM sucrose solution. The two slides face to face were submitted to sinusoidal potential (frequency 10 Hz, amplitude 6 or 9 $V_{p\text{-}p}$) at various temperatures overnight. The temperature was varied from 30°C up to 70°C. In some experiments, to promote the separation of polymersomes from each other and from the slide, a square potential (5 Hz, amplitude 4 $V_{p\text{-}p}$) was applied for one hour. The observation of the sample was then made with an Olympus IX71 microscope.

An alternative set-up was that using the Vesicle Prep device from Nanion. In this case, the protocol was similar, except for the duration of electroformation which was followed by microscopy and was typically 4 hours. The observation was performed using an Olympus BX53 microscope equipped with a x20 LUC plan FLN objective in phase contrast.

**Dynamic light scattering (DLS).** DLS was carried out at 25°C on a Malvern Zetasizer NanoZS equipped with a He-Ne laser (λ=633 nm). Solutions were analyzed as synthesized without filtration to ensure that large populations were not discarded from analysis. Polydispersity indices (**PDI**) were obtained from the correlation function by using a cumulant analysis. The PDI can be useful to give an idea of the polydispersity of the sample and the reliability of the size values. The correlation function was then analyzed *via* the general-purpose non-negative least squares (NNLS) method to obtain the intensity-weighted distribution of diffusion coefficients (D) of the solutes. This distribution can be converted, using Mie theory, to a number-weighted distribution describing the relative proportion of

multiple components in the sample based on their number rather than based on their scattering. The average apparent hydrodynamic diameter, noted as **DLS Size Int or DLS Size Number** in Tables 1-5, were determined using the Stokes-Einstein equation from intensity-weighted and number-weighted distribution respectively. DLS Size Int should be used with care when possible nanoparticle aggregates are present in the solution, since this value will emphasize the large aggregates instead of individual objects. Each solution was analyzed 3-5 times depending on the observed correlogram. The typical accuracy for the measurements was 10-15%. The values presented in the tables are not mean values, because this is not relevant for DLS analysis of multi-population samples. Indeed, in such case, the DLS software will exhibit a larger inaccuracy for the least present population. Thus, the results presented in the tables are those obtained for a typical result for each analysis. All experiments were performed 1-3 times depending on the obtained results. Some led to unsurprising results with clearly defined self-assemblies. These were not necessarily reproduced. Others led to several populations or to unexpected morphologies. These were reproduced and in all cases, the repeated experiments led to very similar results.

The determination of DLS Size Int, DLS Size Number and PDI assumed non-interacting particles modeled as homogeneous hard spheres. Whereas these assumptions might be suitable for nanoparticles and micellar structures, this is clearly not adapted for polymersome samples or mixture of polymersomes and nanoparticles. Therefore, when polymersomes structures are involved, these values might be regarded as relative and are given as indications to facilitate comparison of the different samples. In order to give a critical view on the results of these analyses, a more complete overview of the assumptions relative to these analyses is given in Supporting Information.

**Electron Microscopy**. TEM experiments were performed with a Hitachi HT7700 (Hitachi High Tech, Hitachinaka, Japon) microscope (accelerating voltage of 75 kV). Small amounts of particle suspensions in water were deposited onto a discharged copper grid coated with a carbon membrane, left for 1-3 minutes depending on the solution, and gently dried with absorbing paper. A drop of uranyl acetate solution were deposited onto the grid for 10 seconds, and the grid was then dried under a lamp for at least 5 minutes. When the images contained a large number of distinct objects (typically > 200), a measurement of the mean size (as well as the standard deviation) was performed with Image J software (http://imagej.nih.gov/ij/) and is given in the tables. Cryo-SEM images were performed with a FEG FEI Quanta 250 microscope (Japan). One drop of the sample was frozen in nitrogen slush at -220°C. The frozen sample was transferred under vacuum to the cryo-fracture apparatus (Quorum PP3000T Cryo Transfer System) chamber where it was fractured at -145°C. The temperature was then increased to -95°C and maintained at this temperature during 5 min for sublimation. It was then metalized with Pd for 60 s and introduced into the microscope chamber where it was maintained at -145°C during the observation, operating at 5 kV accelerating voltage.

| Polymer name | $f_{PEO}$ exp | $MCH_2$ | $f_{hydr}$ |
|---|---|---|---|
| PEO5000-PCL33300 | 0.13 | 23940 | 0.37 |
| PEO2000-PCL13300 | 0.13 | 9560 | 0.37 |
| PEO2000-PCL5800 | 0.26 | 6330 | 0.41 |
| PEO2000-PCL8800 | 0.19 | 4820 | 0.45 |
| PEO2000-PCL6700 | 0.23 | 4170 | 0.47 |
| PEO5000-PCL10800 | 0.32 | 7760 | 0.51 |
| PEO2000-PCL2800 | 0.42 | 2010 | 0.52 |
| PEO5000-PCL4000 | 0.56 | 2880 | 0.68 |
| PEO11000-PMMA66500 | 0.14 | 45220 | 0.42 |
| PEO5000-PMMA21500 | 0.19 | 14620 | 0.44 |
| PEO5000-PMMA11900 | 0.30 | 3430 | 0.51 |
| PEO2000-PMMA5040 | 0.28 | 8090 | 0.52 |
| PEO5000-PMMA4100 | 0.55 | 2790 | 0.69 |
| PEO5000-PDLLA20500 | 0.20 | 11380 | 0.55 |
| PEO2000-PDLA5450 | 0.27 | 3020 | 0.59 |
| PEO5000-PDLLA10550 | 0.32 | 5850 | 0.62 |
| PEO10000-PLLA12800 | 0.44 | 7100 | 0.69 |
| PEO10000-PDLLA17650 | 0.36 | 9800 | 0.65 |
| PEO2400-PDLLA2000 | 0.55 | 1110 | 0.75 |
| PCL12300-PEO5000-PCL12300 | 0.17 | 17700 | 0.40 |
| PCL8250-PEO10000-PCL8250 | 0.38 | 11900 | 0.55 |
| PCL4400-PEO10000-PEO4400 | 0.53 | 6300 | 0.66 |

**Table S2**. Calculation of $MCH_2$ and hydrophilic fraction according to Discher[51]

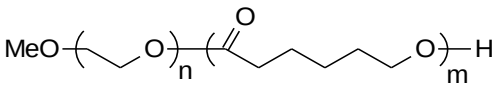


PEO-PCL ($T_g$ PCL = -62°C)

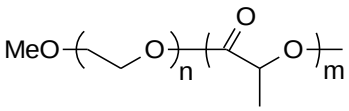


PEO-PDLLA ($T_g$ PDLLA = 50°C)

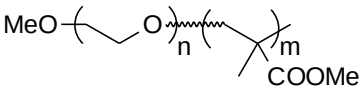


PEO-PMMA ($T_g$ PMMA = 105°C)

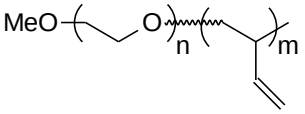


PEO-PBD ($T_g$ PBD range -100 to -15 °C depending on the ratio 1.2 /1.4)

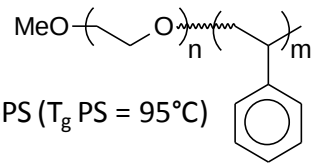


PEO-PS ($T_g$ PS = 95°C)

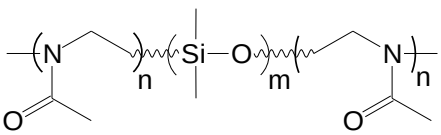


PMOXA-PDMS-PMOXA ($T_g$ PDMS = -123°C)

**Scheme S1.** Polymers used in this study

**TEM for acetone cosolvent method**

PEO5000-PCL33300 normal addition acetone

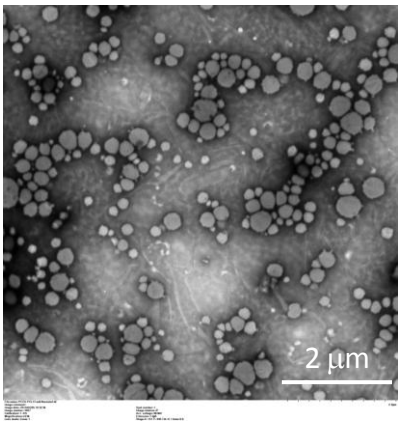


PEO5000-PCL33300 reverse addition acetone

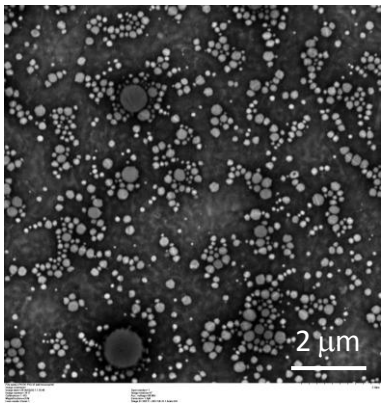


PEO2000-PCL13300 normal addition acetone

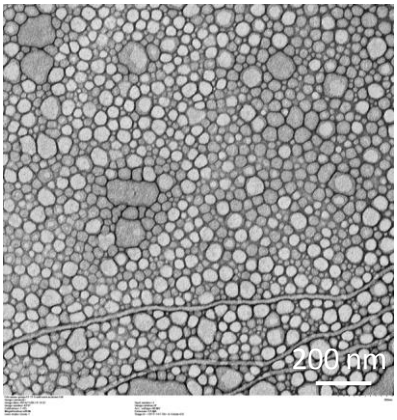


PEO2000-PCL13300 reverse addition acetone

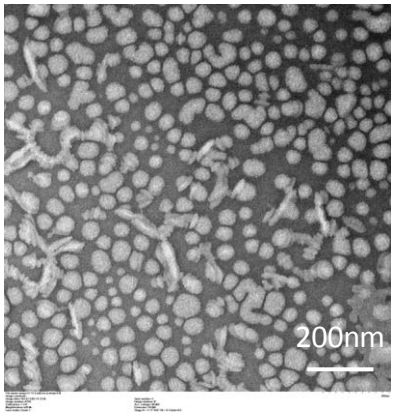


PEO2000-PCL6700 normal addition acetone

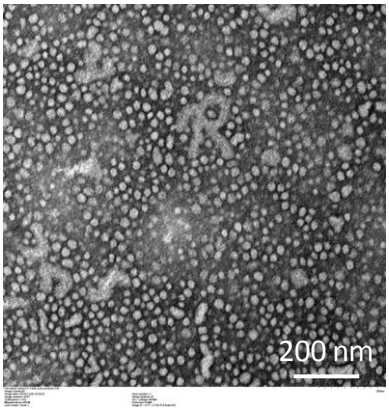


PEO5000-PCL10800 normal addition acetone

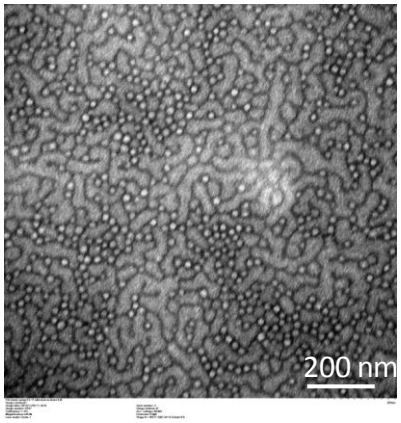

PEO5000-PMMA21500 normal addition acetone

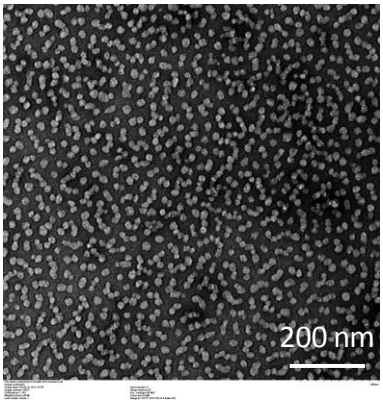


PEO5000-PDLLA20500 normal addition acetone

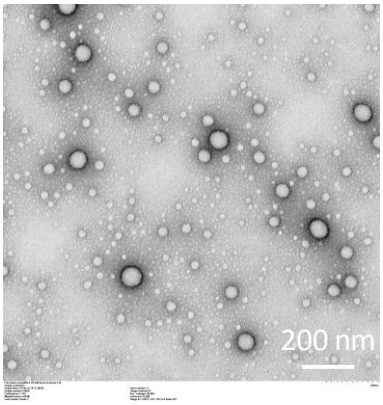


PEO2000-PDLA5450 normal addition acetone

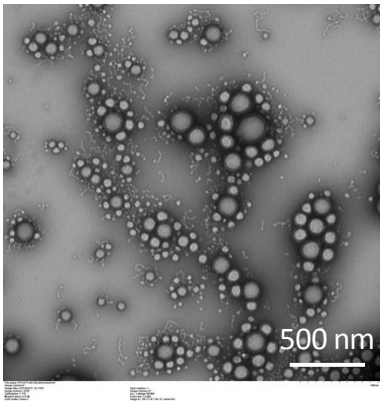


PEO2000-PDLA5450reverse addition acetone

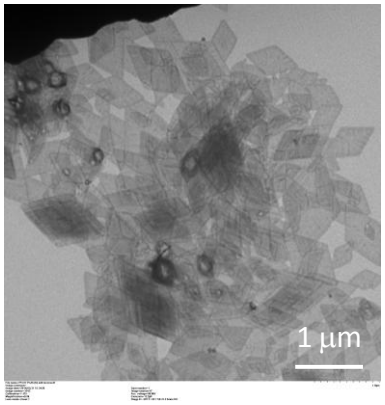

PEO10000-PDLLA17650 normal addition acetone  PEO10000-PDLLA17650 reverse addition acetone

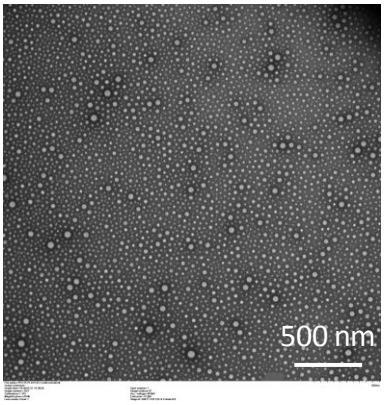


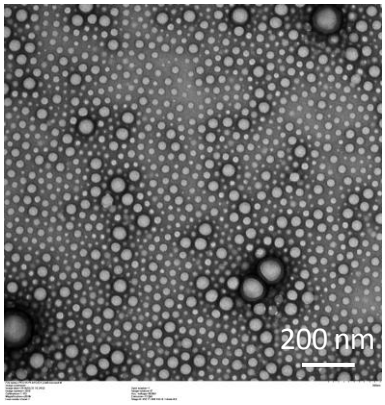


PEO5000-PDLLA10550 normal addition acetone  PEO5000-PDLLA10550 reverse addition acetone

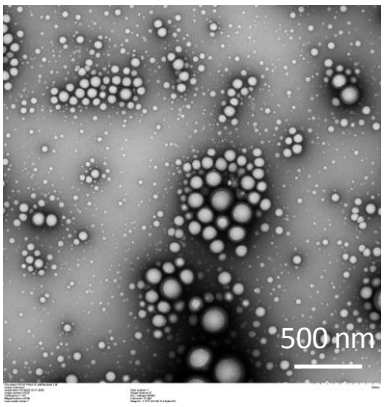


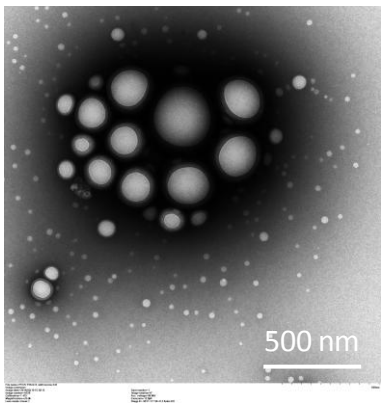


PEO10000-PLLA12800 normal addition acetone  PEO10000-PLLA12800 reverse addition acetone

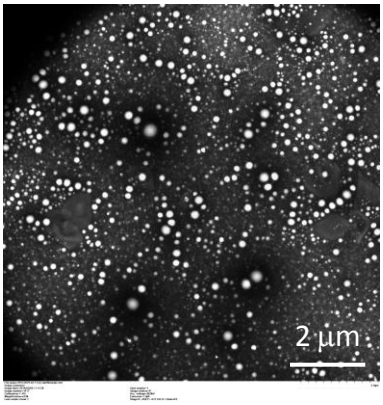


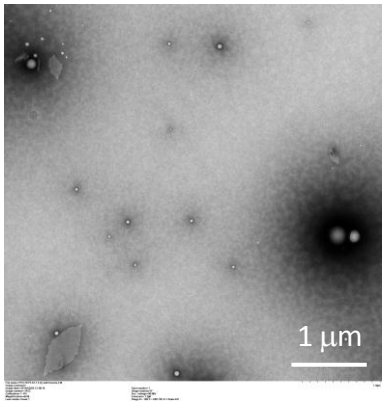

PCL12300-PEO5000-PCL12300 normal addition acetone

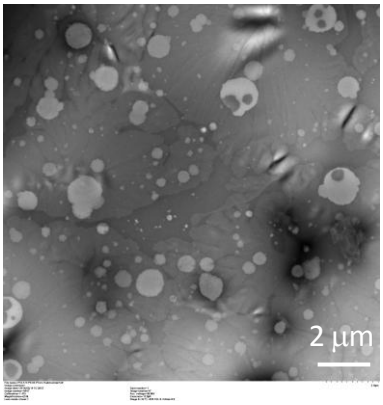


PCL12300-PEO5000-PCL12300 reverse addition acetone

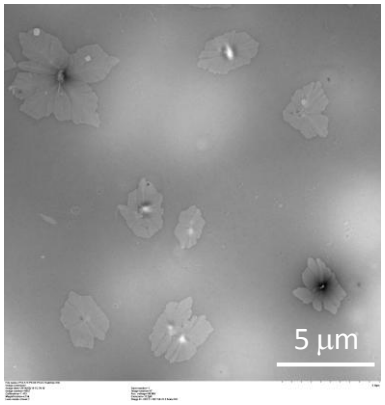


## Acetonitrile cosolvent method

Table S3 presents the results for a few polymers using acetonitrile as a cosolvent. For PEO-PCL polymers, the change of acetone ($\varepsilon$ = 20.7) in acetonitrile ($\varepsilon$ = 37.5) led to a strong decrease of the self-assemblies size, going from 130 to 55 nm for PEO5000-PCL333000. Similar behavior was observed for PEO2000-PMMA5040, when PEO5000-PDLLA20500 presents no significant change between acetone and acetonitrile. Finally, for the triblock copolymer tested, an increase of the dispersity was recorded due to the appearance of a new population of smaller nano-objects. Therefore, in general, acetonitrile seems to lead to slightly smaller aggregates than acetone. Different behaviors according to the organic solvent are often linked to the interaction parameter between the polymer chains and the solvent or the solvent dielectric constant. Here, no clear relation between these parameters and the objects sizes differences appears when changing from acetone and acetonitrile. This makes us confirm that object formation is under kinetic control when the organic solvent is added to water. PEO-PS self-assemblies could not be formed in this manner owing to insolubility of the initial copolymer in acetonitrile.

| Polymers | $f_{PEO\ exp}$ | DLS Size Int (nm) | DLS Size Number (nm) | PDI | Mean size from TEM (nm) | Morphology from TEM |
|---|---|---|---|---|---|---|
| PEO5000-PCL33300 | 0.13 | 110 | 55 | 0.3 | 57 ± 49 | Polymersomes / micelles ? |
| PEO2000-PMMA5040 | 0.28 | 40 | 24 | 0.2 | | Micelles* |
| PEO5000-PDLLA20500 | 0.19 | 194 | 128 | 0.1 | 21 ± 9 | Micelles |
| PCL12300-PEO5000-PCL12300 | 0.30 | 880/220 | 680/210 | 0.5 | | Particles |

**Table S3**. Results obtained from "Acetonitrile cosolvent" method using the addition of acetonitrile onto water.

*no TEM performed, morphology suggested only from DLS size

**Interaction parameters of the polymer blocks**

| Polymer | THF | Acetonitrile | Acetone | eau |
|---|---|---|---|---|
| PCL | $(0.13)_{100°C}$ | | $(0.46\text{-}0.54)_{100°C}$ | |
| PMMA | 0.46-0.49 | 0.5 (25°C) | 0.48 | |
| PDLLA | | | $(0.56)_{120°C}$ | |
| PS | 0.4 | 2 pour $\phi$ proche de 1 et 160°C | 0.6-0.8<br>Butanone 0.5 | |
| PBD | | | | 3.5 |
| PEO | $(0.3)_{100°C}$ | | $(0.47)_{100°C}$ | 0.45 |

$\chi$ <0 miscible

0 < $\chi$ <0.5 good solvent

$\chi$ = 0.5 $\theta$ condition

$\chi$ > 0.5 poor solvent

From the handbook of polymer-liquid interaction parameters and solubility parameters. Allan F.M. Barton, CRC Press, Boca Raton.1990

PEO5000-PCL33300 normal addition acetonitrile

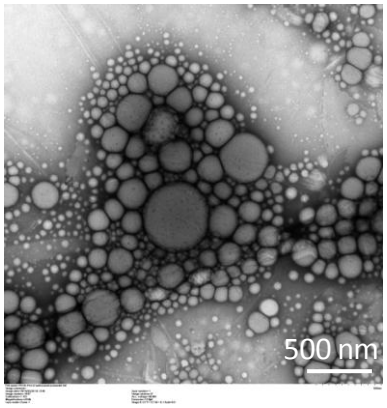


PCL12300-PEO5000-PCL12300 normal addition acetonitrile

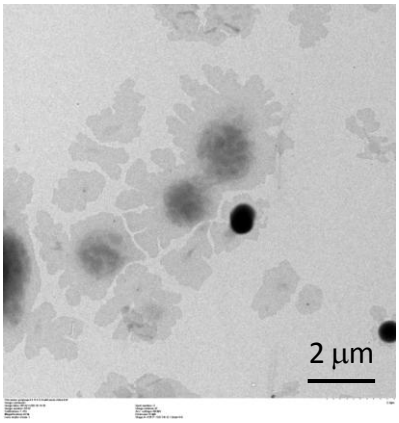


PEO5000-PDLLA20500 normal addition acetonitrile

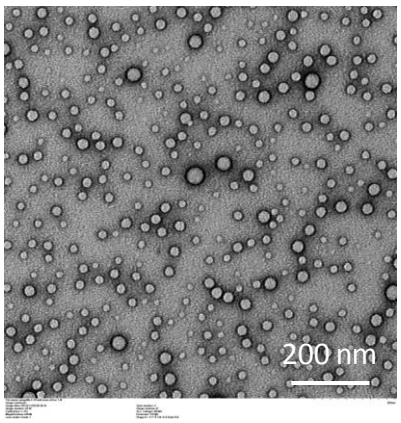

**TEM for "THF/MeOH cosolvent method"**

PEO2000-PCL13300 reverse addition Water/BA onto THF/MeOH

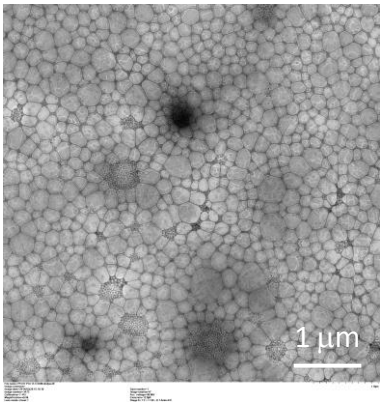


PEO2000-PCL5800 reverse addition Water/BA onto THF/MeOH

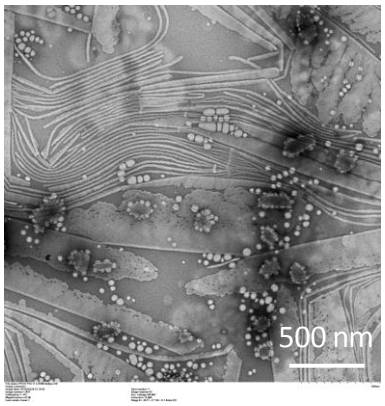


PEO2000-PCL8800 reverse addition Water/BA onto THF/MeOH

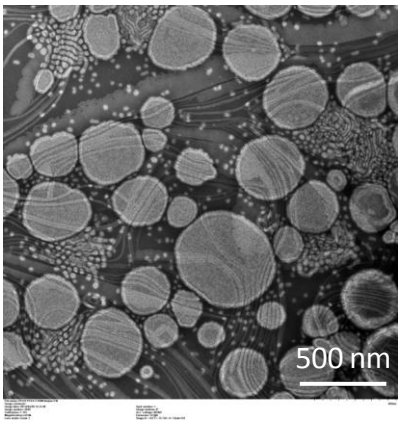


PEO15000-PS37300 reverse addition Water/BA onto THF/MeOH

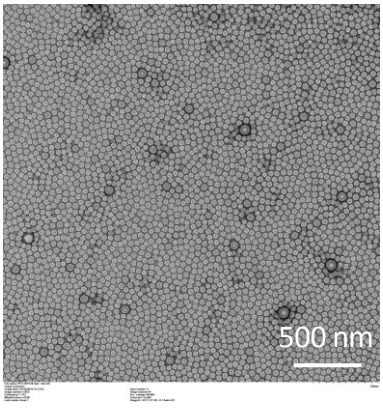


PEO2000-PMMA5040reverse addition water/BA onto THF/MeOH

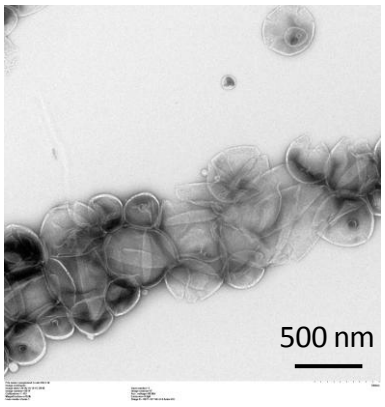

PEO3900-PBD6700 reverse addition water/BA onto THF/MeOH

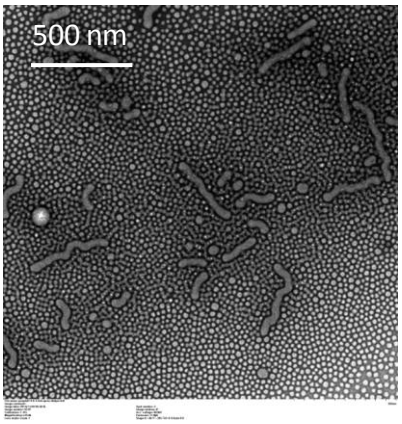


PEO5000-PDLLA20500 reverse addition water/BA onto THF/MeOH

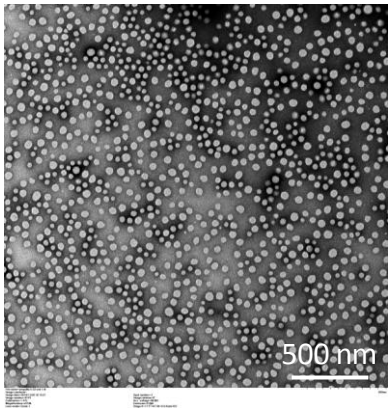


**TEM for "Meng method"**

PEO2000-PCL6700 Meng

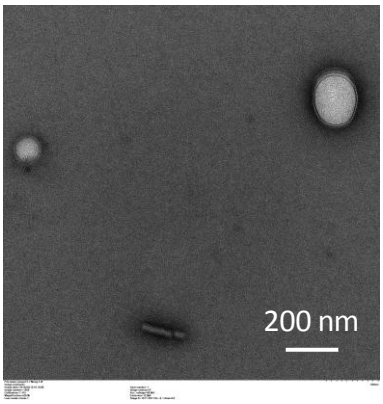


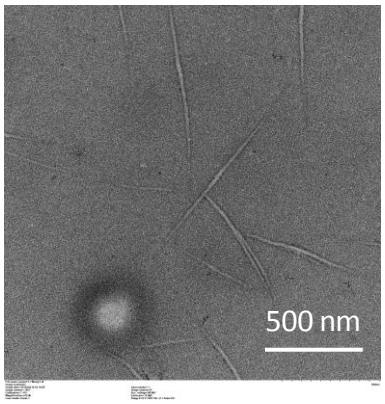


PEO2000-PCL13300 Meng

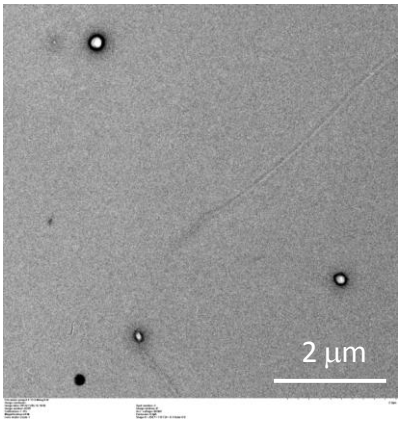


PEO5000-PDLLA20500 Meng

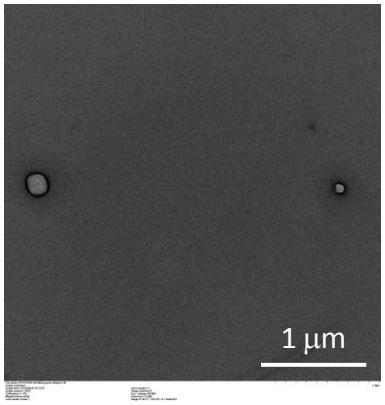

PEO2000-PMMA5040 Meng

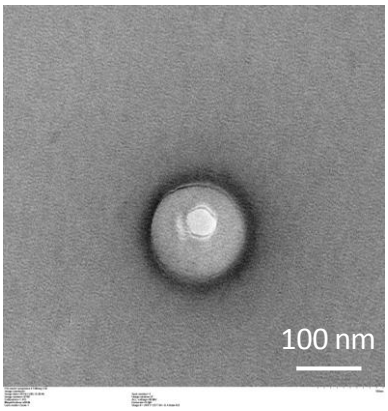


PEO5000-PDLLA10550 Meng

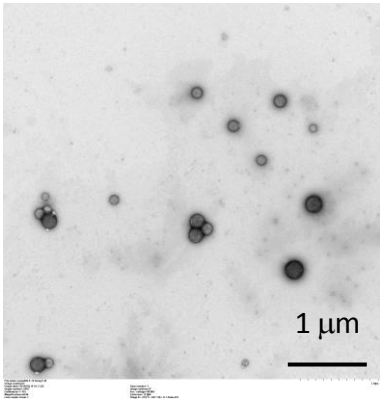


PEO5000-PDLLA20500 Meng

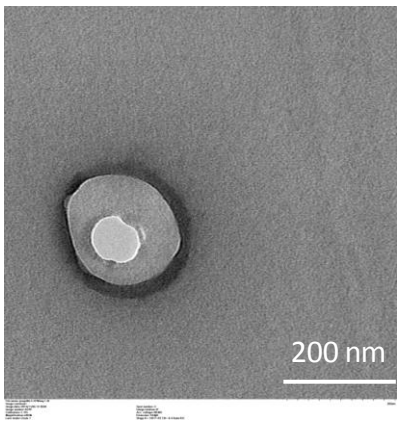


PEO3900-PBD6700 Meng

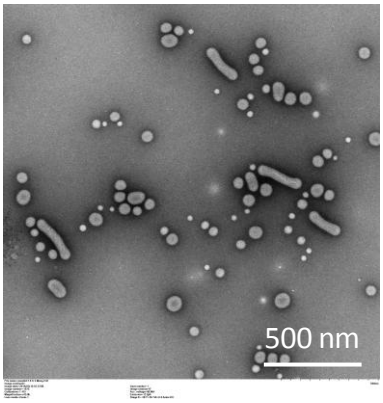

PCL12300-PEO5000-PCL12300 Meng

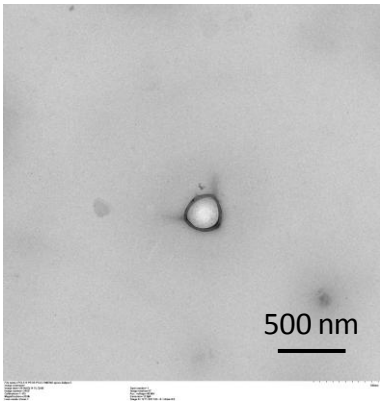


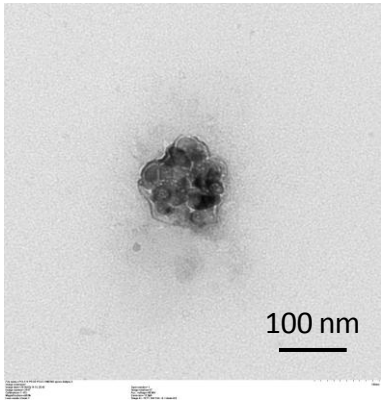


**TEM for film rehydration method**

PEO2000-PCL6700 film rehydration

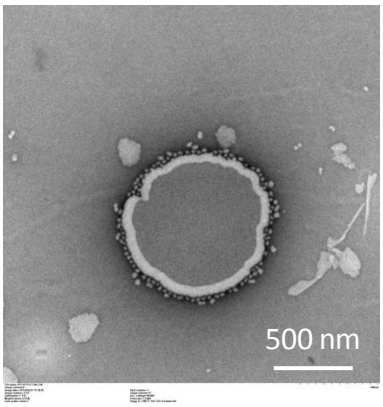


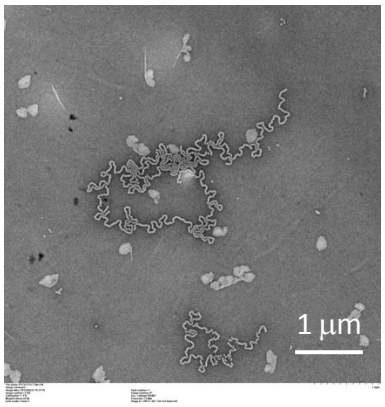


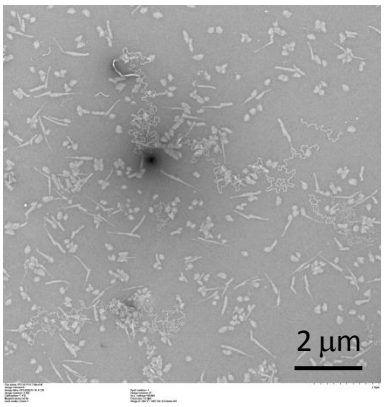


PEO5000-PCL10800 film rehydration

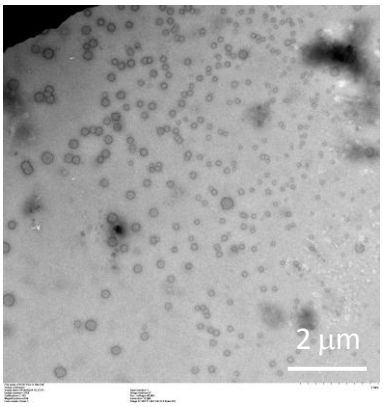


PEO2000-PCL13300 film rehydration

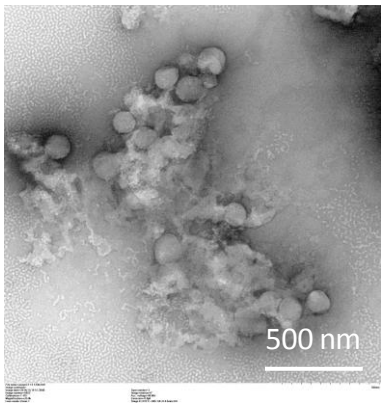

PEO2000-PCL8800 film rehydration

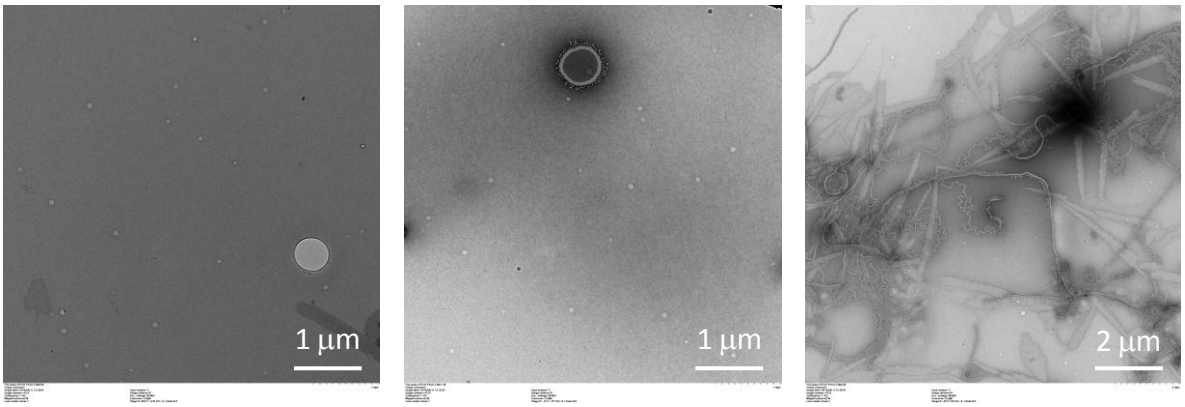


PCL12300-PEO5000-PCL12300 film rehydration

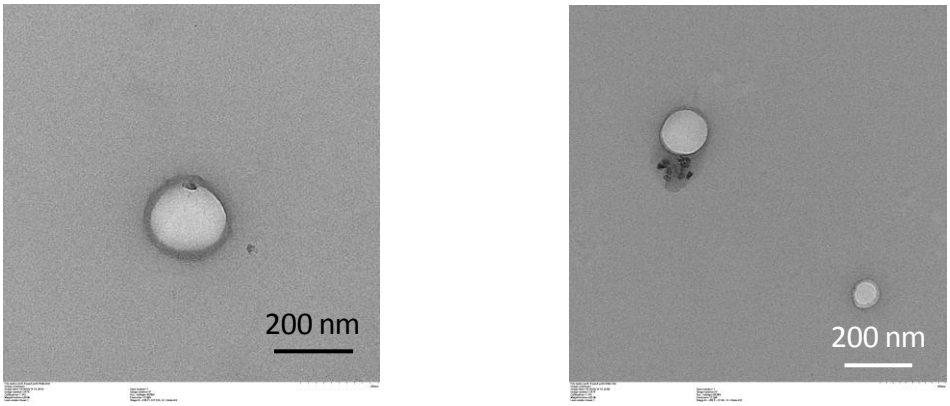


PEO3900-PBD6700 film rehydration

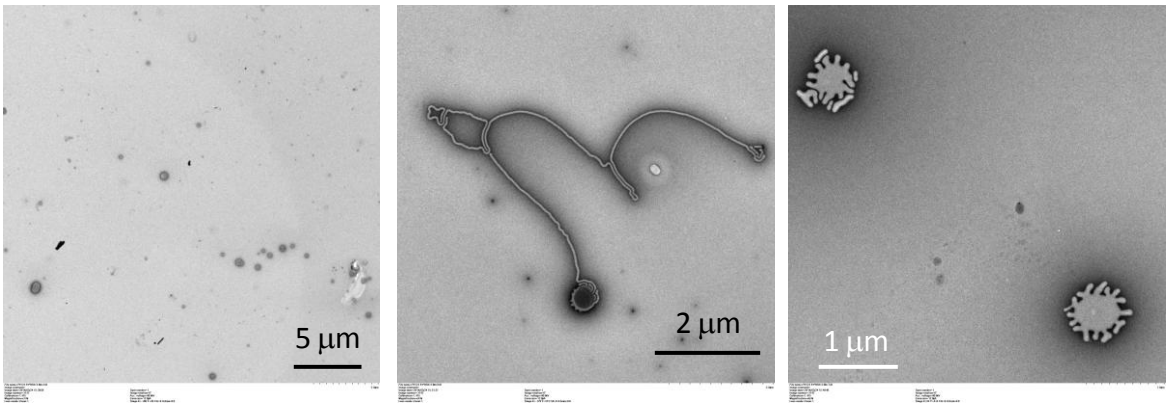

**Prevision of self-assembly morphologies**. The principles that govern the self-assembly of amphiphilic molecules can be related, in a first approach, to simple geometric arguments. The formation of a specific structure (micellar, vesicles,…) is controlled by the relative size (or weight fraction) of hydrophilic to hydrophobic segments. This parameter determines the curvature of the hydrophilic-hydrophobic interface and therefore the membrane in the 3 dimensions, represented by the two radii of curvature $R_1$ and $R_2$. In the 1980s, Israelachvili developed a model based on pure geometrical considerations to predict morphologies of self-assemblies of small molecules. This model is based on the definition of a packing parameter p linking the hydrophobic volume v to the interfacial area a and the hydrophobic chain length l (Israelachvili, J. N. et al. Physical principles of membrane organization. *Quaterly Reviews of Biophysics* **1980**, *13*, 121) , which is also related to the radii $R_1$ and $R_2$:

$$p = \frac{v}{al} = 1 - \frac{l}{2}\left(\frac{1}{R_1} + \frac{1}{R_2}\right) + \frac{l^2}{3R_1R_2}$$

Depending on the values of p, different morphologies are formed i.e. $0 < p < 1/3$: spherical micelles in aqueous media, $1/3 < p < 1/2$: cylindrical micelles, $1/2 < p < 1$: lamellar systems and $p > 1$: reverse self-assemblies.

**Weight fraction ($f_{EO\ m}$) and volume fraction ($f_{EO\ vol}$)** of PEO can be calculated from each other by the following equations:

$$f_{EO\ m} = \frac{f_{EO\ vol} * \rho_{EO}}{\rho_{pol} + f_{EO\ vol} * (\rho_{EO} - \rho_{pol})}$$

$$f_{EO\ vol} = \frac{f_{EO\ m} * \rho_{pol}}{\rho_{EO} + f_{EO\ m} * (\rho_{EO} - \rho_{pol})}$$

where $\rho_{EO}$ and $\rho_{pol}$ are respectfully PEO density and the hydrophobic block melt density (Won, Y.-Y. et al. Cryogenic Transmission Electron Microscopy (Cryo-TEM) of Micelles and Vesicles Formed in Water by Poly(ethylene oxide)-Based Block Copolymers. *The Journal of Physical Chemistry B* **2002**, *106*, 3354; Ahmed, F. et al. Self-porating polymersomes of PEG-PLA and PEG-PCL: hydrolysis-triggered controlled release vesicles. *J. Controlled Release* **2004**, *96*, 37).

**PCA analysis. Data analysis.** *S*tatistical evaluation of data was performed using principal component analysis (PCA, P. C. Jurs, G. A. Bakken and H. E. McClelland, Chem. Rev. 2000, 100, 2649-2678). PCA is a statistical procedure using an orthogonal transformation to convert a set of observations of possibly correlated variables into a set of values of linearly uncorrelated variables. These new sets are the eigenvectors of the covariance matrix of the initial set and are linear combinations of the original variables. They are also called principal components. The first principal component contains the maximum information (i.e. variance) from the initial data set, and each succeeding component accounts for the maximum remaining variance of the data set. PCA analysis enables to reduce the dimensionality of a data set by using only the first few principal components that contains the maximum information (i.e. variance). Therefore, plots of principal component enable to obtain a lower-dimensional picture of the original data and can reveal relationships, such as natural data clustering, differentiation and outliers. In this article, all data analysis was performed using a macro for excel software. Standardized values were obtained for each variable from the divison of measured values by corresponding standard deviation (in order to have a variance equal to one for all variables). These values were then used for data treatment by PCA.

**A. Principal components (PC) and associated variance**

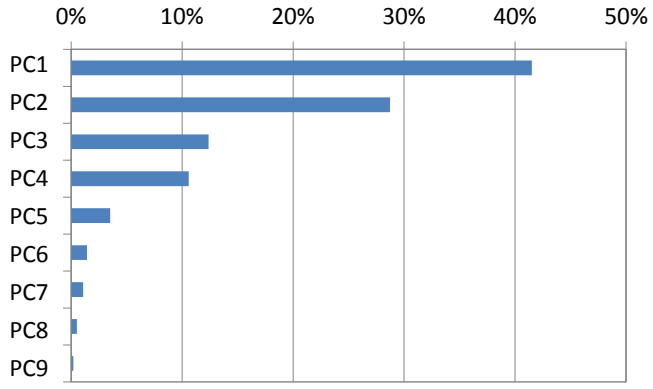


**B. Correlation between the different variables**

| | Mn (SEC) | Mn,hydrophilic | Mn,hydrophobic (1H NMR) | fPEO | DLS Size Int (nm) | DLS size Number (nm) | PDI | TEM Size | TEM standard deviation |
|---|---|---|---|---|---|---|---|---|---|
| $M_n$ (SEC) | 1 | 0,68348499 | 0,889381188 | -0,3171585 | -0,066342578 | -0,116094678 | 0,15484473 | 0,02952784 | -0,037110274 |
| $M_{n,hydrophilic}$ | 0,68348499 | 1 | 0,5994682 | 0,245494609 | -0,076691777 | -0,175258014 | 0,05479332 | -0,11369625 | -0,119443395 |
| $M_{n,hydrophobic}$ ($^1$H NMR) | 0,88938119 | 0,5994682 | 1 | -0,47153677 | -0,014955745 | -0,041367296 | 0,1638357 | 0,12505808 | 0,086558106 |
| $f_{PEO}$ | -0,3171585 | 0,245494609 | -0,471536773 | 1 | -0,243783875 | -0,264956979 | -0,0139529 | -0,34056494 | -0,412801413 |
| DLS Size Int (nm) | -0,06634258 | -0,076691777 | -0,014955745 | -0,24378387 | 1 | 0,943661763 | -0,10765449 | 0,93327499 | 0,79892506 |
| DLS size Number (nm) | -0,11609468 | -0,175258014 | -0,041367296 | -0,26495698 | 0,943661763 | 1 | -0,20185204 | 0,88146136 | 0,684523564 |
| PDI | 0,15484473 | 0,054793319 | 0,163835705 | -0,0139529 | -0,10765449 | -0,201852037 | 1 | -0,0169608 | -0,036196432 |
| TEM Size | 0,02952784 | -0,113696252 | 0,125058076 | -0,34056494 | 0,93327499 | 0,881461356 | -0,0169608 | 1 | 0,827174722 |
| TEM standard deviation | -0,03711027 | -0,119443395 | 0,086558106 | -0,41280141 | 0,79892506 | 0,684523564 | -0,03619643 | 0,82717472 | 1 |

**C. Correlation between the two principal components and initial variables** (horizontal axis: first principal component, PC1; vertical axis: second principal component, PC2.)

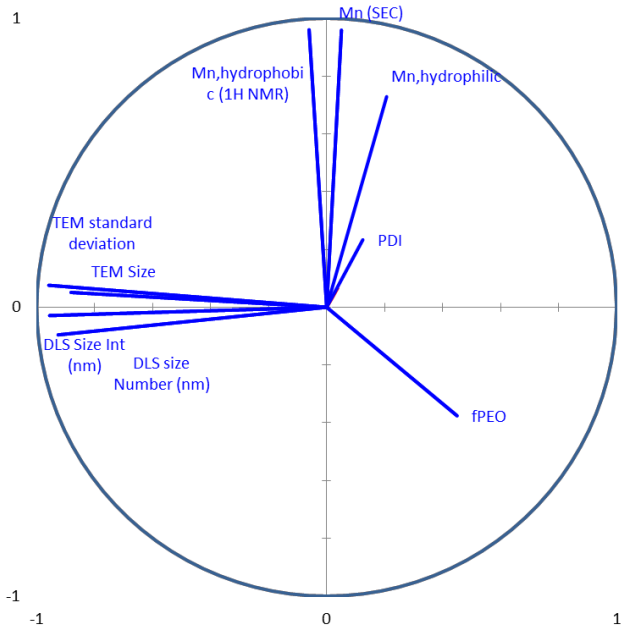


## D. Score plot with sample name

PCA score plot from self-assemblies obtained by using different methods of formation from different families of block copolymer. The first principal component is positively correlated to the hydrophilic fraction and negatively correlated with size obtained from DLS or TEM whereas the second principal component is positively correlated with measured average molecular weights (from SEC or NMR) and PDI and negatively correlated with hydrophilic fraction. Legend: P: polymersome, M: Micelle, N nanoparticle, W: wormlike.

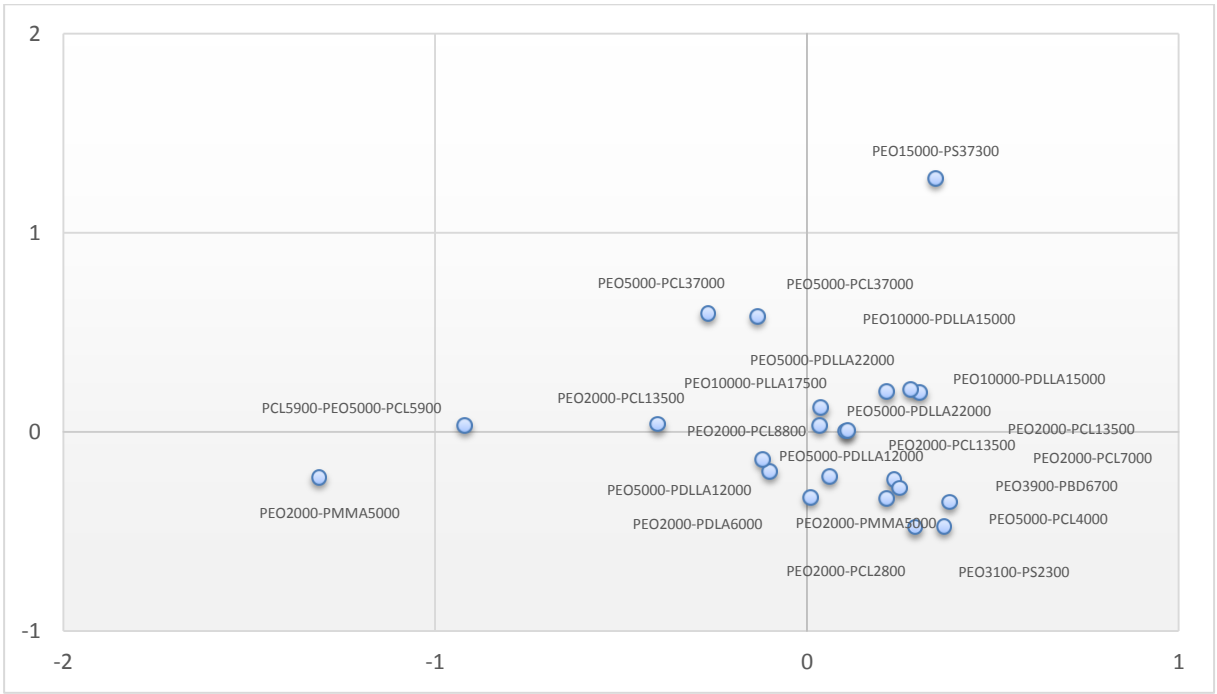


**Figure S1. Complementary results of PCA for Figure 3.**

A second PCA analysis was performed by considering only samples issued from method 1. For this analysis, only sizes obtained from DLS measurements were used. The conclusion from this second set of data led to the same conclusion than the first set that include all methods and size measured from TEM analysis.

**A. Score plot for samples issued from first preparation method**

(horizontal axis: first principal component, PC1; vertical axis: second principal component, PC2, correlations were given on the following graph.)

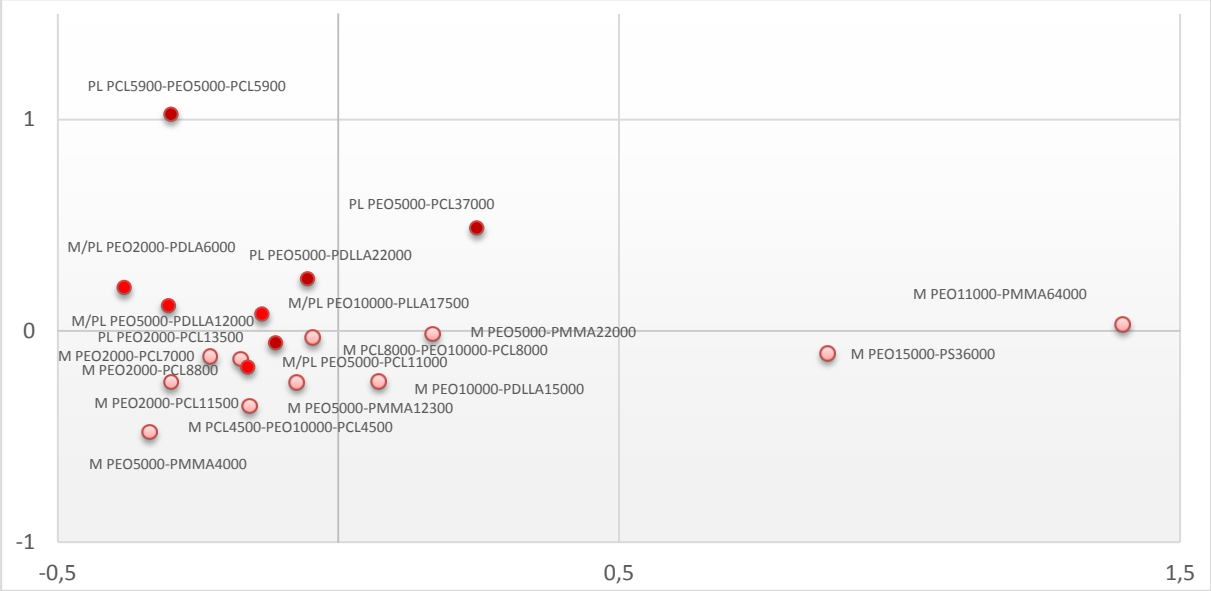


**B. Correlation between the two principal components and initial variables** (horizontal axis: first principal component, PC1; vertical axis: second principal component, PC2.)

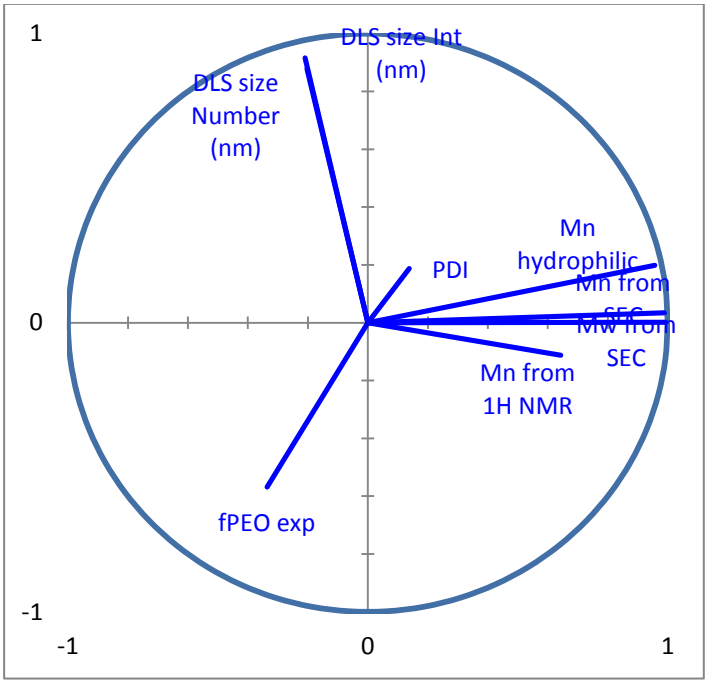

**Special cases of "PEO5000-PCL75000" and "PEO1400-PMMA5600"**

Among all polymers received, these were found to be very different from the announced polymer. First, "PEO5000-PCL75000" was found to be a mixture of PEG, PEO-PCL and homo-PCL. "PEO1400-PMMA5600" contained a non-negligible proportion of a polymer that could not be identified, containing presumably polyesters, and possibly aldehyde moieties. Although these polymers were not described in the main text of the manuscript, we believe it is of interest to discuss their ability to form nano-objects in parallel of the main study.

| Polymers | $f_{PEO\ th}$ | Method | DLS Size Int (nm) | DLS Size Number (nm) | PDI | Mean size from TEM (nm) | Morphology from TEM |
|---|---|---|---|---|---|---|---|
| "PEO5000-PCL75000" | 0.16 | Normal addition acetone | 300 | 200 | 0.1 | 65.6 ± 58.5 | Polymersomes / NP? |
| | | Reverse addition acetone | 270 | 140 | 0.2 | 133.9 ± 73.5 | Polymersomes / NP? |
| | | Normal addition acetonitrile | 130 | 70 | 0.2 | | Polymersomes / micelles* ? |
| | | THF/MeOH | 290 | 190 | 0.2 | 106.0 ± 110.4 | Polymersomes / NP? |
| | | Meng | 280 | 170 | 0.2 | | Micelles / Polymersomes |
| | | Rehydration | 290 | 70 | 0.3 | | Polymersomes / micelles* ? |
| "PEO1400-PMMA5600" | 0.2 | Normal addition acetone | 500 | 360 | 0.2 | | Polymersomes aggregates |
| | | Normal addition acetonitrile | 840 | 300 | 0.4 | | Polymersomes ? |
| | | THF/MeOH | 330 | 330 | 1.0 | | Polymersomes* ? |
| | | Meng | | 230 (cryo-SEM) | | | Polymersomes or NP ? |

* no TEM performed, morphology suggested only from DLS size

Comparing the formation of nano-objects for "PEO5000-PCL75000" with the other copolymers, one can observe that its behavior is close to that of PEO5000-PCL37000. Thus, in this case, the presence of a large amount of homopolymer does not modify the type of objects observed. In this case, cryo-TEM images showed the presence of very dense particles with a small internal cavity.

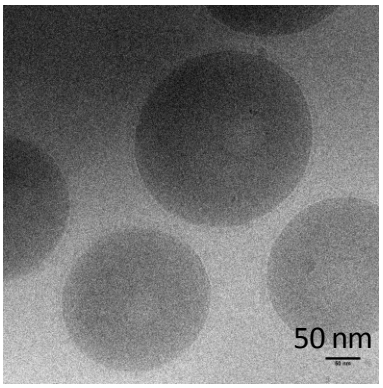


cryo-TEM “PEO5000-PCL75000” inverse addition using acetone.

As for the case of impure “PEO1400-PMMA5600”, the presence of the side product is in this case fundamental for the formation of nano-objects. Formation of large self-assemblies, typically associated to polymersomes, was systematic for this polymer, whereas the use of PEO2000-PMMA5000 more often led to micelles or smaller polymersomes comparing similar conditions.

impure PEO1400-PMMA5600 normal addition acetone

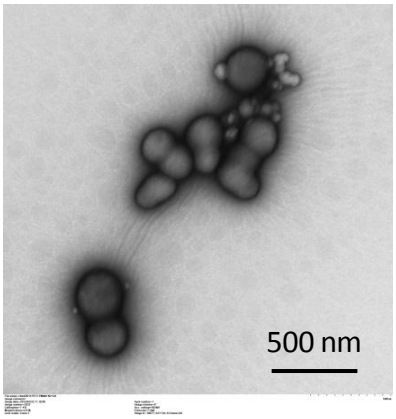


impure PEO-PMMA 1400-5600 normal addition acetonitrile

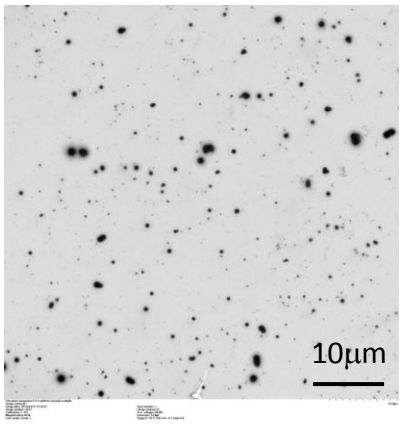

“PEO-PCL 5-75” normal addition acetone

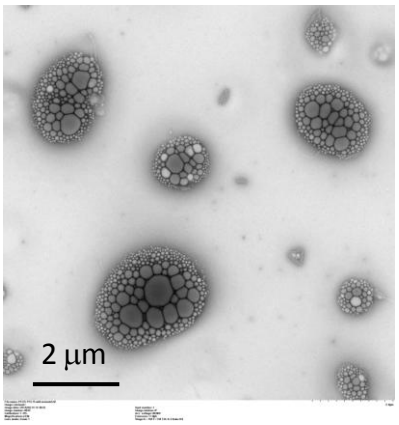


“PEO-PCL 5-75 “reverse addition acetone

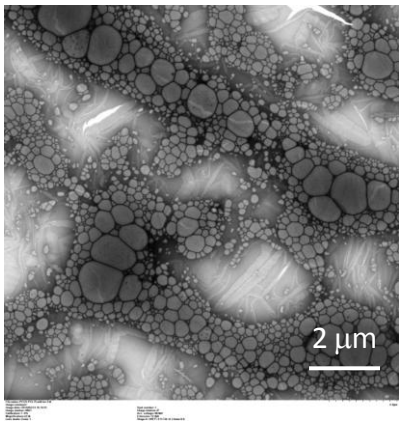


“PEO-PCL 5-75” reverse addition Water/BA onto THF/MeOH

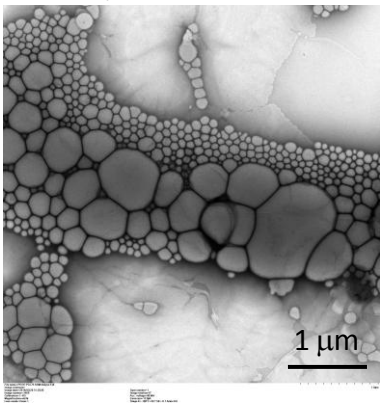


“PEO-PCL 5-75” Meng

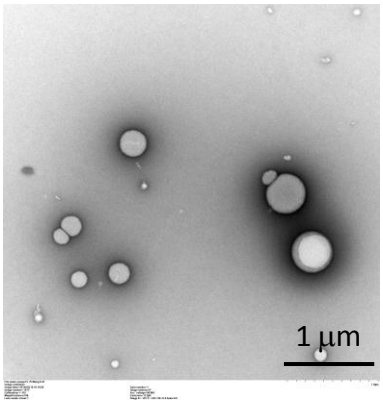

**Theoretical background of Dynamic Light scattering (DLS).**

DLS analysis was used to extract Z-average values, derived count rate, intensity and number average distributions for each studied nano-object sample. In order to give a critical view on the results issued from these analyses, a brief overview of the assumptions relative to these is given below.

**From auto-correlation function to self-diffusion coefficient D.** Particles in suspension (without sedimentation or creaming) undergo random Brownian motion with a characteristic (translational) diffusion coefficient D, which is related to the size and shape of the objects (see below). Under laser illumination, this motion induces a random fluctuation of the light scattered by the particles. The temporal behavior of the intensity of the scattered light contains therefore information on the particles' size and shape. To extract this information, analysis through auto-correlation of the scattered intensity signal could be performed. The auto-correlation intensity function $G(\tau,q)$ is defined as followed :

$$G(\tau,q) = \langle I(t,q).I(t+\tau,q)\rangle / \langle I(t,q)\rangle^2 \quad \textbf{(1)}$$

with <> denotes the integral of the function versus the time t
$\tau$ the delay time,
q the scattering vector $q = 4\pi n/\lambda_o \sin(\theta/2)$ with $\lambda_o$ the incident laser wavelength, $\theta$ the scattering angle and n the optical index of the solution.

In the following parts, we suppose that each photon is scattered only once before being detected i.e. the solutions are diluted enough. When multiple scattering occurs, the results below are no longer correct.

In the case of *monodisperse and non-interacting nanoparticles,* $G(\tau,q)$ is following a single exponential decay:

$$G(\tau,q) = A.(1+\beta.[e^{-\Gamma.\tau}]^2) \quad \textbf{(2)}$$

with A the measured baseline,
$\beta$ a parameter depending on the coherence optics,
$\Gamma$ is a decay rate, which is equal to $q^2.D$ .

Fitting the auto-correlation function of the experimental scattered intensity leads therefore to an estimation of the diffusion coefficient. Then, the size of the particle may be estimated from D after making assumption on the shape of the object. In the simple case of spherical particles, one will use the Stokes-Einstein equation:

$$R_h = k_B T/(6\pi\eta D) \text{ (Stokes Einstein)} \quad \textbf{(3)}$$

with $R_h$ the hydrodynamic radius,
$\eta$ the viscosity of the solution at the temperature T,
$k_B$ the Boltzmann constant.

Note that the hydrodynamic radius is influenced by any changes of the nanoparticles surface structure or concentration of ions in the medium and that any mistake on the used viscosity and optical index values induces an important error on the calculated $R_h$. For anisotropic objects, the single exponential decay of the auto-correlation function is still observed for not so long objects (typically less than 150 nm). For such particles, various models have been developed to estimate a geometrical parameter of the particles (generally the length assuming

a particular thickness over length ratio) from the translational diffusion (see JACS 2006, 128(5), 1639 and J Chem. Phys. 2003, 119, 8, 9914 for nanorods, Macromolecules 1979, 12(2), 320 for wormlike micelles, J. Chem. Phys. 2004, 121 (18), p 9111 for ellipsoids…). For longer objects, the auto-correlation functions are no more a single exponential decay and are influenced by both the translational and rotational diffusion coefficients (J. Chem. Phys. 1968, 48, 4126, Langmuir 2000, 16, 1689). Finally, whatever the geometry of the nanoparticles may be, the diffusion coefficient is affected by the concentration of particles, i.e. by the interparticle interactions. In the simplest form, the measured diffusion coefficient will follow (J. Phys. Chem. B, 2004, 108, 7021):

$$D = D_o.(1+k.\Phi_{eff}) \quad \textbf{(4)}$$

with $D_0$ the hydrodynamic radius without interparticle interactions,
k a constant, equal to 1.56 in the case of monodisperse hard spheres,
$\Phi_{eff}$ the effective volume fraction of particles.

Furthermore, the normalized average quantity of photon reaching the correlator (**Derived count rate** in the Malvern software) is a valuable indication to avoid misinterpretation issued from the single analysis of auto-correlation function. A low value for this quantity indicates either a too low concentrated sample or the absence of significant amount of colloidal structures within solution. It also renders the treatment of auto-correlation function more risky as the level of relative noise is dramatically increased.

In the case of *polydisperse and non-interacting nanoparticles,* the auto-correlation intensity function $G(\tau,q)$ no longer follows a single exponential decay but should be based on a sum or an integral over a distribution $F(\Gamma)$ of the diffusion coefficient:

$$G(\tau,q) = A.(1+\beta.[\int_0^\infty F(\Gamma).e^{-\Gamma.\tau}\ d\Gamma\ ]^2) \text{ with } \int_0^\infty F(\Gamma)\ d\Gamma = 1 \quad \textbf{(5)}$$

Note that this distribution is over the decay rate not over the size of particles.
The main difficulty is now to extract from the experimental autocorrelation function, the distribution function $F(\Gamma)$. Two approaches can be used:

- if the distribution function is monomodal and narrow enough, one can use the cumulant analysis leading to the **Z-average diameter** and an estimate of the width of the distribution (**Polydispersity index PDI**).

- in the general case, one can estimate the distribution function by a discrete function. Fitting this function with the auto-correlation one will lead to a plot of the relative intensity of light scattered by particles in various size classes (**intensity size distribution**).

**Determination of polydispersity by cumulant analysis.** Using Taylor expansion and cumulants of the distribution function, one can demonstrate that the equation (5) leads to (Applied Optics 40(24) 4087 (2001):

$$G(\tau,q) = A(1+\beta.e^{-2\bar{D}.q^2\tau}.\left(1+\frac{\mu_2}{2!}.\tau^2-\frac{\mu_3}{3!}.\tau^3\ldots\right)^2) \quad \textbf{(6)}$$

with $\bar{D}$ the average hydrodynamic diffusion coefficient,
$\mu_i$ the i th moment of the distribution function F defined as:
$\mu_i = \int_0^\infty F(\Gamma).(\Gamma - q^2.\bar{D})^i.d(\Gamma)$ .

Fitting the experimental auto-correlation to the equation (6) by the least squares method gives easily:

- the average hydrodynamic diffusion coefficient which corresponds to the mean of the distribution F(Γ), assuming a single peak Gaussian distribution. The equivalent hydrodynamical diameter (through the Stokes Einstein equation, with the hypothesis that the nanoparticles are spherical – i.e. micelles, vesicles, polymersomes etc…-) can then be calculated and is called the intensity weighted **Z-average mean diameter.** The Z-average mean diameter is the recommended value to be used in quality control (ISO standard document 13321:1996 E and 22412). If the sample is not a solution of monomodal, spherical and monodisperse nanoparticle, the Z-average size can only be used to compare various samples measured in the same dispersant and same conditions.
- the value second moment ($\mu_2$) leads to the **polydispersity index** corresponding to the relative standard deviation of that distribution (PdI). In the case of a Gaussian distribution, this is directly the variance of the distribution. If estimated, the third moment ($\mu_3$) provides a measure of the skewness or asymmetry of the distribution.

**Fit of the correlation function by multiple exponential: intensity size distribution.** For *samples with a multiple size distribution*, G(τ,q) is written as a discreet sum of exponential functions:

$$G(\tau,q) = A.(1+\beta.[\sum_i \alpha_i . e^{-\Gamma_i \cdot \tau} \, d\Gamma]^2) \qquad \textbf{(7)}$$

with $\alpha_i$ the intensity-weighted contribution of the $\Gamma_i$ decay rate associated to particles having a diffusion coefficient of $D_i = \frac{\Gamma_i}{q^2}$. The intensity-weighted distribution is obtained from a deconvolution of the measured intensity autocorrelation function of the sample. Generally, this is accomplished by using a non-negatively constrained least squares (NNLS) fitting algorithm, common examples being CONTIN, General Purpose and Multiple Narrow Mode algorithms using a certain number of defined size classes. These different algorithms differed from each other by the level of noise which is kept before deconvolution process (also called regularization). Indeed, a small amount of noise in the correlation function can generate a large number of distributions. In the case of spherical homogeneous particles, the intensity-weighted particle size distribution is then obtained by using Stokes Einstein equation (3).

**From intensity distribution to volume or number size distribution**. The intensity distribution is naturally weighted according to the scattering intensity of each particle fraction or family. As such, the intensity distribution can be somewhat misleading, in that a small amount of aggregation or presence or a larger particle species can dominate the distribution. This distribution can be converted, using Mie theory, to a number distribution describing the relative proportion of multiple components in the sample based on their number rather than based on their scattering. Given the optical properties of the particle and the scattering angle, Mie theory estimates the scattering intensity M(x) as a function of particle diameter x, dispersant and particle optical properties. The discreet list of $\Gamma_i$ decay rate associated weighted by $\alpha_i$ could be transformed into a list of radii $R_i$ (assuming spherical particles) through the equation $D_i = \frac{\Gamma_i}{q^2} = k_B T/(6\pi\eta R_i)$ weighted by the coefficient $\alpha_I/M(R_i)$.

Alternatively, conversion can be roughly obtained by assuming that M(x) is proportional to $R^6$ (in the case of small homogeneous spheres – i.e. micelles but not vesicles or polymersomes -) which is only correct for particle below ca 100 nm of diameter. For vesicles or polymersomes, one may suppose that M(x) is proportional to $R^4.t^2$ where t is the thickness of the shell thickness (JICS 165, 512 (1994)). Note that the Mie theory implies that a particular model has been chosen to describe the particles (homogeneous, spheres, hollow spheres, coated spheres…).

When transforming an intensity distribution to a number distribution, different assumptions are used: *all particles are homogeneous and spherical, the optical properties of the particles are known and intensity distribution is correct*. Moreover DLS technique itself produces distributions with inherent peak broadening, so there will always be some error in the representation of the intensity distribution. As such, number distributions derived from these intensity distributions emphasizes information obtained from a small fraction of the collected data. Therefore they are best used for comparative purposes, or for estimating the relative proportions where there are multiple modes, or peaks, and should never be considered as absolute.

**Determination of intensity and number average distributions, polydispersity for studied polymersome sample**. To further illustrate how dynamic light scattering data have been used within this study to determine different structural parameters (noted as '**DLS Int**', '**DLS Number**', '**PDI**' in the main text), we present below DLS data obtained from PEO2000-PCL13300 colloidal solutions. As stated above, it has to be remembered that polymersome are hollow sphere and therefore inhomogeneous materials. Thus, DLS results could not be considered as absolute values and are taken for comparison purpose.

In this study different methods of self-assembly formation were examined: acetone addition onto water, water addition onto acetone, Water/benzyl alcohol addition onto THF/MeOH, Meng method, film rehydration. Correlograms obtained from these preparations are illustrated on the Figure below:

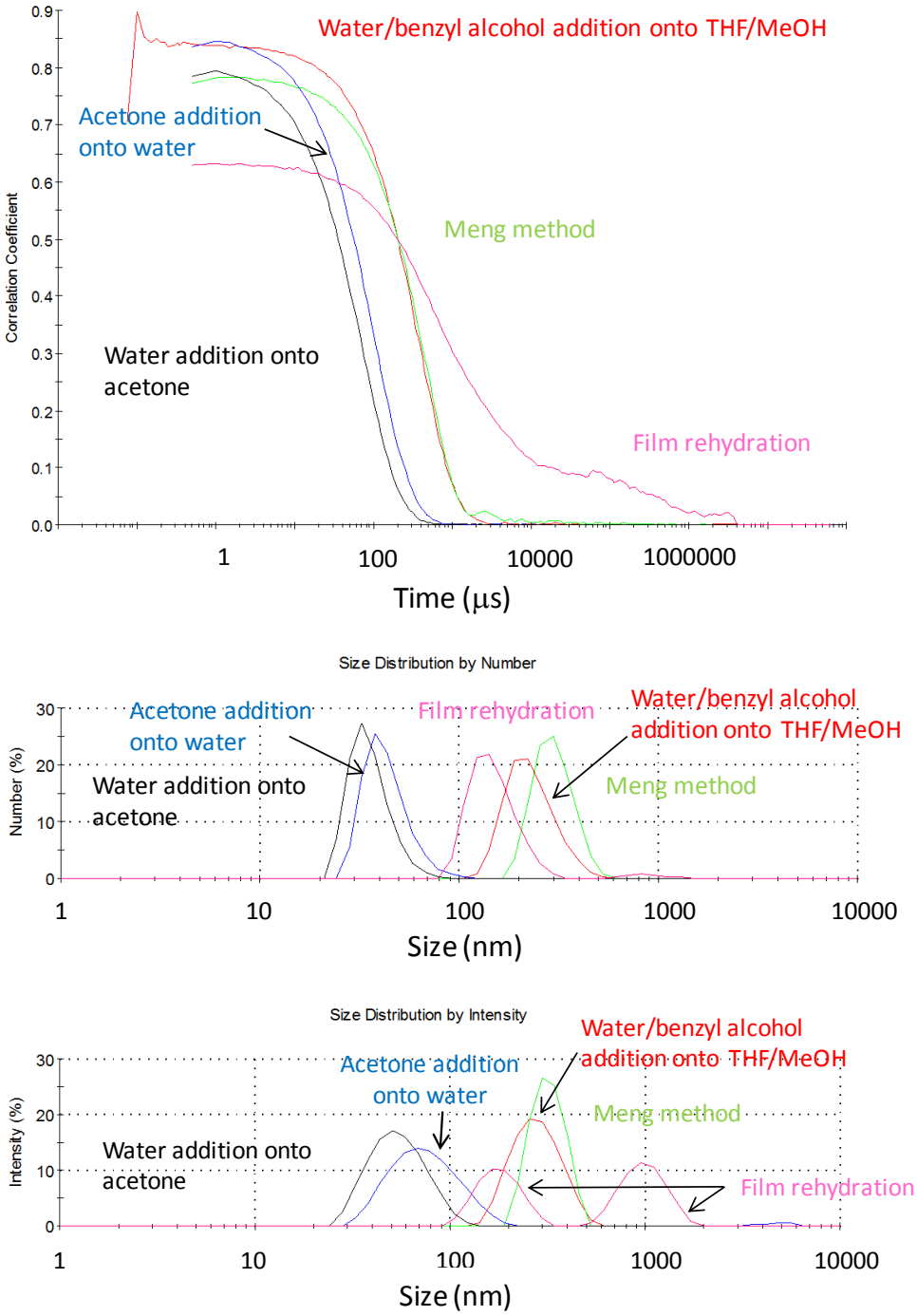


**Figure S2.** Correlation function illustrating different preparation methods for PEO2000-PCL13300 self-assembly structures and corresponding distribution average size in intensity or in number.

A first look at the different correlograms gave us the most important trends of this comparative study. As the correlograms are significantly different, preparation methods clearly greatly influence the final structure of obtained nanoobjects:

- Acetone addition onto water and water addition onto acetone preparation methods led to rather similar correlograms corresponding to average intensity size of 80 and 55 nm respectively (noted **DLS Int in the main text**).

- A right shift of correlograms is observed for water/benzyl alcohol addition onto THF/MeOH or Meng preparation methods related to the formation of larger objects in solution with an average intensity size of 280 and 320 nm respectively.
- Lastly, the lower slope observed after the first plateau on the correlogram issued from film rehydration method indicated an increased of size polydispersity. Moreover, for this sample, the presence of a second plateau suggested the formation of larger object. Thus the rehydration method led to polydisperse and polymododal structures.

**DLS Size Int**, **DLS Size Number** and **PDI** were obtained from these correlograms by an analysis using general purpose algorithm for DLS Int, DLS Number and a cumulant analysis for PDI. Both approaches assumed spherical hard sphere models. Whereas this assumption might be suitable for nanoparticles and micellar structures, this is clearly not adapted for polymersome samples or mixture of polymersomes and nanoparticles. Therefore, when polymersomes structures were involved, these values might be regarded as relative value and are given as indicative values to facilitate comparison of the different samples.

**Typical optical microscopy photographs of electroformed polymersomes**

PEO3900-PBD6700 12V, 50°C, 10Hz

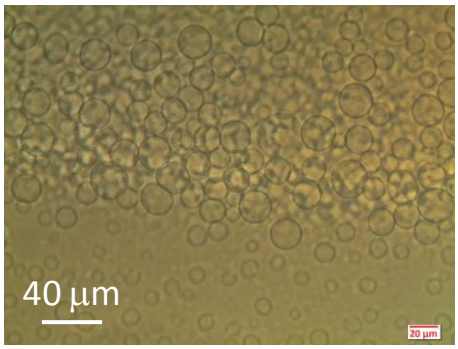


PMOXA1500-PDMS4500-PMOXA1500 12V, 10Hz, 70°C

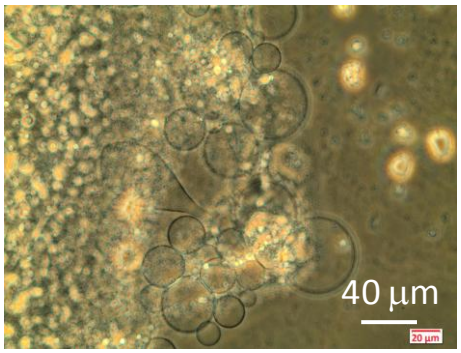


PEO3900-PBD6700 6V, 50°C, 10Hz

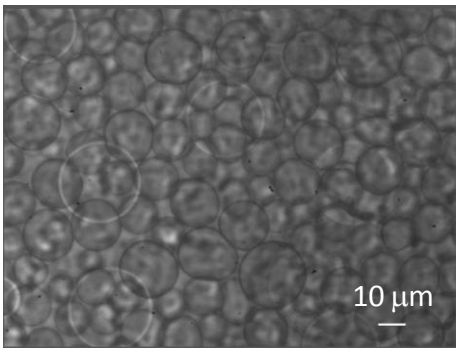


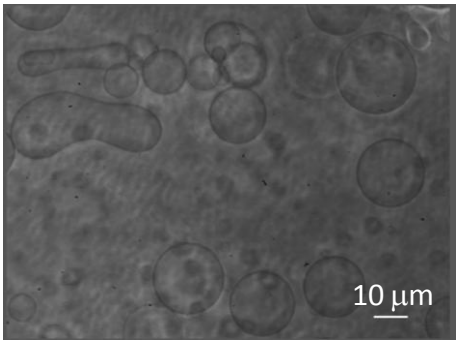


PEO3900-PBD6700 6V, 50°C, 10Hz formed in the presence of 50mM sucrose